Distributed Recursive State Estimation Over Sensor Networks With Compress-and-Forward Relays: A Compressed Sensing Strategy

Pengyu Wen, Zidong Wang, Hongli Dong, and Weihao Song

***Abstract*—This paper addresses the distributed recursive state estimation problem for wireless sensor networks operating under stringent energy, bandwidth, and computational constraints. A compress-and-forward relay architecture integrated with compressed sensing is proposed to reduce the transmission burden while preserving the information required for reliable estimation. Within the proposed framework, sensor measurements are compressed at the relay and reconstructed at the remote estimator from low-dimensional observations. To account for the uncertainty induced by wireless transmission, the effects of channel fading and channel noise on the compressed-sensing reconstruction process are analysed, and a corresponding reconstruction error model is established by exploiting channel statistical characteristics. On this basis, a distributed recursive state estimator is developed to mitigate channel-induced distortion. An upper bound on the estimation error covariance is then derived in the presence of reconstruction error, and the estimator gains are determined by minimizing this bound. Simulation studies based on an unmanned surface vehicle mooring-assisted dynamic positioning system demonstrate that the proposed method can maintain satisfactory estimation accuracy and robustness while significantly reducing communication overhead.**

***Index Terms*—Distributed state estimation; wireless sensor networks; compress-and-forward relay; compressed sensing; recursive estimation; channel fading; unmanned surface vehicle.**

I. INTRODUCTION

State estimation is regarded as a fundamental component of modern technological systems, by which internal system states are inferred from sensor measurements and mathematical models when direct observation is not available. Such a capability is required in a broad range of critical applications, including precise navigation for autonomous underwater vehicles, smart industrial automation, and real-time monitoring in environmental sensing and offshore energy systems [3], [9], [14], [42], [49], [51]. Over recent decades, substantial progress has been achieved in estimation and filtering theory, leading to statistically optimal solutions for diverse scenarios. Among the available methods, the Kalman filter has been recognized as one of the cornerstones of linear estimation. Its recursive prediction-and-update structure is well known for optimally fusing uncertain system dynamics with noisy measurements so that minimum mean-square-error estimates can be obtained. Owing to its robustness and computational efficiency, the Kalman filter has been widely adopted as a fundamental framework for state estimation in numerous engineering fields, as extensively documented in the literature [19], [34], [37], [41], [44].

Recent advances in networking and wireless communication technologies have made sensor networks a predominant architectural framework for distributed monitoring and control. Considerable attention has been devoted to such networks because several practical advantages can be offered simultaneously, including simplified wiring, reduced cost, flexible deployment, convenient scalability, and easier maintenance [30], [31], [39], [44]. Owing to these merits, sensor networks have been widely adopted in large-scale application scenarios such as ocean monitoring, forest fire detection, and precision agriculture [4], [6], [22], [23], [47]. In such scenarios, geographically dispersed sensing units can be organized in a cooperative manner, so that information from different locations can be collected and transmitted without requiring rigid physical interconnections. Such a distributed architecture makes sensor networks particularly attractive in environments where centralized wiring is costly, deployment conditions are harsh, or system expansion is frequently required. For this reason, sensor networks have become an indispensable technical foundation for many modern monitoring and control systems.

It is noted that practical large-scale deployment is severely restricted by the limited resources available at sensor nodes. Energy scarcity remains one of the most prominent concerns, because battery-powered nodes possess only restricted energy budgets, while the repeated transmission of high-dimensional raw data is highly energy-intensive and can drastically shorten network lifetime [15]. Bandwidth limitation in wireless channels further aggravates the problem, since the transmission of

This work was supported in part by the Provincial Key Research and Development Program of Heilongjiang Province of China under Grant 2024ZXJ01A04, in part by the Royal Society of the UK, and in part by the Alexander von Humboldt Foundation of Germany. (*Corresponding author: Hongli Dong.*)

Pengyu Wen is with the Key Laboratory of Continental Shale Hydrocarbon Accumulation and Efficient Development, Ministry of Education, Northeast Petroleum University, Daqing, Heilongjiang 163318, China. (Email: pengyuwen_nepu@163.com).

Zidong Wang is with the Department of Computer Science, Brunel University of London, Uxbridge, Middlesex, UB8 3PH, U.K. (Email: Zidong.Wang@brunel.ac.uk).

Weihao Song is with the School of Advanced Manufacturing and Robotics, Peking University, Beijing 100871, China, and also with the Department of Computer Science, Brunel University of London, Uxbridge, Middlesex, UB8 3PH, U.K. (Email: Weihao.Song@brunel.ac.uk).

Hongli Dong is with the Artificial Intelligence Energy Research Institute, Northeast Petroleum University, Daqing, Heilongjiang 163318, China. (Email: shiningdhl@vip.126.com).

massive raw data is likely to suffer from congestion, significant delay, and high packet-loss rates. Meanwhile, the weak computational capability of sensor nodes often makes complex local data processing impossible in real time [45]. Under the combined constraints of energy, bandwidth, and computation, direct transmission of large raw data streams to a distributed estimator becomes highly inefficient and often impractical [20], [40], [43]. To ensure reliable state estimation under such conditions, intermediary nodes with data-processing capability should be introduced into the network architecture, so that the burden on the sensor-to-estimator link can be alleviated. Relay nodes are therefore strategically employed to form the communication backbone. The effectiveness of such a relay-assisted architecture, nevertheless, depends strongly on the adopted relaying strategy, since different relaying mechanisms do not address the above constraints with the same efficiency.

Remote state estimation scenarios usually involve measurement signals transmitted over long-distance communication channels [8], [48], [50]. Because of the limited transmission power of sensors and the unavoidable fading of wireless signals, direct communication with a remote estimator often experiences severe path loss. Relay techniques are therefore indispensable for reliable communication [21], [26], [35]. Among the predominant relaying protocols, amplify-and-forward is attractive because of its low complexity, yet both signal and noise are amplified simultaneously, which inevitably degrades estimation performance [46]. Decode-and-forward can suppress noise propagation by fully decoding and re-encoding the received signal, but substantial computational resources are required at the relay, resulting in increased latency and energy consumption. Such a drawback is particularly critical in resource-constrained sensor networks [36]. The compress-and-forward (CF) strategy adopted in this work provides a more balanced alternative. In CF relaying, the received signal is compressed at the relay without full decoding, and the data volume as well as bandwidth usage can thereby be reduced, while the noise amplification associated with amplify-and-forward and the heavy computational burden caused by decode-and-forward are both avoided [1], [10]. For bandwidth-limited and energy-limited scenarios, CF is therefore especially suitable. Efficient compression with minimal information loss, nevertheless, remains a pivotal issue in conventional CF relay frameworks.

Efficient compression in the CF paradigm can be effectively addressed through compressed sensing (CS), which has emerged as a powerful signal-processing framework. By exploiting the fact that many natural signals are sparse or compressible in a known transform domain, such as the discrete cosine transform or wavelet domain, CS breaks away from the limitations imposed by the traditional Nyquist-Shannon theorem. Rather than acquiring the full signal as in conventional schemes, CS employs a non-adaptive and signal-independent measurement matrix to obtain a small number of linear projections at a rate far below the Nyquist rate [5], [11], [28], [38]. Provided that sufficient sparsity is present, the original signal can be accurately reconstructed at the remote estimator by solving an appropriate convex optimization problem. Such a property makes CS highly attractive for CF relays [16]. The implementation burden at the relay is low, since compression mainly involves a simple matrix-vector multiplication, and this feature makes CS well suited to resource-constrained nodes [33]. Moreover, CS is essentially signal-agnostic, because its effectiveness depends on the existence of sparsity rather than on any particular signal type. The design of complicated application-specific compression codes can thus be avoided [24]. Owing to its universality and strong compression capability, CS provides an effective means for integrating data compression and communication in CF relay systems.

Motivated by the above discussion, in this paper, we investigate the state estimation problem for wireless sensor networks (WSNs), where a CF relay integrated with CS techniques is adopted, by which highly efficient data compression can be achieved at the relay. Within the proposed framework, three core issues are addressed. i) The first concerns the establishment of a CF relay model compatible with CS techniques. ii) The second concerns the analysis of the effect of multiplicative random fading in wireless channels on the accuracy of CS recovery, because the compressed signals become stochastic and partially unknown under such fading, and a reliable compression error model must therefore be constructed. iii) The third concerns the design of an appropriate state estimator for processing the compressed-and-recovered signals generated by the CS-based relay framework, so that the overall effectiveness and robustness of system state estimation can be ensured. The main contributions of this paper are summarized as follows.

1) For the first time, the CF relay architecture is systematically introduced into the state estimation problem for resource-constrained WSNs, and a CF relay design integrated with CS techniques is investigated. Compared with traditional CF relay schemes, the proposed approach can effectively exploit CS technology to significantly reduce the number of required measurements while preserving the estimation performance.
2) One of the first systematic investigations of the influence of stochastic channels on CS recovery error is provided in this work. By exploiting channel statistical characteristics rather than instantaneous channel state information, a state estimator is designed to counteract the uncertainty induced by wireless channels.
3) The effectiveness of the designed estimator is rigorously validated through simulations based on an unmanned surface vehicle (USV) mooring-assisted dynamic positioning system (MADPS). The results demonstrate the practical applicability of the proposed approach in a realistic scenario.

The remainder of this paper is organized as follows. Section II establishes a discrete time-varying sensor network under a CF relay with CS techniques, analyzes the influence of channel statistics on the CS recovery error, and develops the corresponding distributed recursive state estimator. Section III presents the distributed state estimation scheme by minimizing an upper bound of the estimation error covariance. Section IV provides a simulation case study of a USV-MADPS to verify the effectiveness of the proposed approach. Section V concludes the paper.

Notation: $\mathbb{R}^m$ stands for the m-dimensional Euclidean space. $A > 0$ represents that A is a positive definite symmetric matrix. For a square matrix B, $\mathrm{tr}(B)$ illustrates the trace of B. $\mathbb{E}\{a\}$ and $\mathbb{V}\{a\}$ show the expectation and the variance of the random variable a, respectively. The symbol $\ll$ means "much less than" and is used to indicate that one quantity is significantly smaller than the other.

II. Problem Formulation and Preliminaries

A. System Description

In this paper, a sensor network containing N sensor nodes is considered, whose topology is described by a specified directed graph $\mathbf{G} = (\Theta, \Xi, \Lambda)$ of order N with the set of nodes $\Theta = \{1, 2, \ldots, N\}$, the set of edges $\Xi \subseteq \Theta \times \Theta$, and the weighted adjacency matrix $\Lambda = [a_{ij}]_{N\times N}$ with adjacency elements $a_{ij} \geq 0$. An edge of $\mathbf{G}$ is represented by pair (i, j). The adjacency elements associated with the edges of the graph are positive, i.e., $a_{ij} > 0 \Longleftrightarrow (j, i) \in \Xi$, which indicates that information is transmitted from sensor j to sensor i. The set of neighbors of node i is denoted by $\mathbf{N}_i = \{j \in \Theta : a_{ij} > 0\}$ $(j \neq i)$.

Consider a class of discrete time-varying sensor networks as follows:

$$\begin{cases} x_{s+1} = A_s x_s + B_s \omega_s \\ y_{i,s} = C_{i,s} x_s + D_{i,s} v_{i,s}, \quad i = 1, \ldots, N \end{cases} \tag{1}$$

where $x_s \in \mathbb{R}^{n_x}$ and $y_{i,s} \in \mathbb{R}^{n_y}$ are state and measurement output of the i-th node, respectively. The vectors $\omega_s \in \mathbb{R}^{n_\omega}$ and $v_{i,s} \in \mathbb{R}^{n_v}$ are noise sequences with zero mean and covariance $Q_s > 0$ and $R_{i,s} > 0$, respectively. A_s, B_s, $C_{i,s}$ and $D_{i,s}$ are known matrices with appropriate dimensions. Throughout this paper, all noise processes and stochastic variables involved are assumed to be mutually uncorrelated and independent across nodes.

1) Compress-and-Forward Relay Channel: In this paper, a communication scheme employing a CF relay is adopted to improve the transmission quality and extend the propagation distance between sensors and remote estimators. As shown in Fig. 1, the sensor measurements are transmitted to the corresponding remote estimators through the CF relays. The end-to-end transmission process consists of two cascaded wireless channels and is described as follows:

2) Sensor-to-relay transmission: The sensor acquires time-domain measurements $y_{i,s}$ and transmits them to the relay through a wireless channel:

$$z_{i,s}^S = \sqrt{p_i^S} h_{i,s}^S y_{i,s} + \eta_{i,s}^S \tag{2}$$

where p_i^S denotes the average transmit power of the sensor node, $h_{i,s}^S \sim \mathcal{N}(\bar{h}_i^S, \tilde{h}_i^S)$ is the sensor-to-relay channel parameter, and $\eta_{i,s}^S \in \mathbb{R}^{n_y}$ is the additive channel noise vector with $\|\eta_{i,s}^S\|_2 \leq \bar{\eta}_i^S$.

3) Compressive sensing at relay: It is assumed that the sensor measurement $y_{i,s}$ admits a sparse representation in a known transform domain. Specifically, $y_{i,s}$ can be expressed as

$$y_{i,s} = \Psi_i \mathbf{s}_{i,s} \tag{3}$$

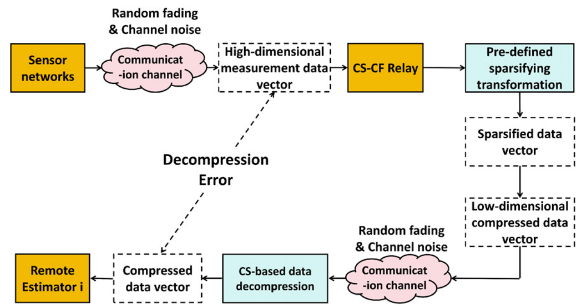

Fig. 1: Framework of CF relay-based transmission under the CS techniques.

where $\Psi_i \in \mathbb{R}^{n_y \times n_y}$ is a known sparsifying basis (e.g., the discrete fourier transform matrix), and $\mathbf{s}_{i,s} \in \mathbb{R}^{n_y}$ is a K-sparse coefficient vector satisfying $\|\mathbf{s}_{i,s}\|_0 \ll K \ll n_y$.

The CF relay applies a CS scheme to $z_{i,s}^S$ and acquires a compressed measurement vector given by

$$z_{i,s}^C = \Phi_i z_{i,s}^S + \eta_{i,s}^C \tag{4}$$

where $\Phi_i \in \mathbb{R}^{n_\Phi \times n_y}$ denotes the compressive sensing matrix with $n_\Phi \ll n_y$, $\eta_{i,s}^C$ represents the compression noise satisfying $\|\eta_{i,s}^C\|_2 \leq \bar{\eta}_i^C$ and $\bar{\eta}_i^C$ is typically related to the hardware conditions during actual compression. This framework enables signal reconstruction from n_Φ compressed measurements instead of the original n_y-dimensional observations. To guarantee unique and stable recovery, the sensing matrix Φ_i is required to satisfy the Restricted Isometry Property (RIP), which is defined as follows.

Definition 1: ([5]) A matrix Φ satisfies the RIP of order K if there exists a scalar $\delta_K \in (0, 1)$ such that for all K-sparse vectors $\mathbf{x}$:

$$(1 - \delta_K)\|\mathbf{x}\|_2^2 \leq \|\Phi\mathbf{x}\|_2^2 \leq (1 + \delta_K)\|\mathbf{x}\|_2^2. \tag{5}$$

The smallest constant δ_K satisfying (5) is called the K-restricted isometry constant.

4) Relay-to-estimator transmission: The relay forwards only the compressed vector $z_{i,s}^C \in \mathbb{R}^{n_\Phi}$ to the remote estimator, whereby the bandwidth requirement is reduced by a factor of $n_y - n_\Phi$. The received signal at the estimator is then given by

$$\begin{aligned} z_{i,s}^R &= \sqrt{p_i^R} h_{i,s}^R z_{i,s}^C + \eta_{i,s}^R \\ &= \sqrt{p_i^R} h_{i,s}^R (\Phi_i z_{i,s}^S + \eta_{i,s}^C) + \eta_{i,s}^R \\ &= \sqrt{p_i^R} h_{i,s}^R (\Phi_i (\sqrt{p_i^S} h_{i,s}^S y_{i,s} + \eta_{i,s}^S) + \eta_{i,s}^C) + \eta_{i,s}^R \\ &= \sqrt{p_i^R p_i^S} h_{i,s}^R h_{i,s}^S \Phi_i y_{i,s} + \eta_{i,s} \end{aligned} \tag{6}$$

with

$$\eta_{i,s} \triangleq \sqrt{p_i^R} h_{i,s}^R \Phi_i \eta_{i,s}^S + \sqrt{p_i^R} h_{i,s}^R \eta_{i,s}^C + \eta_{i,s}^R$$

where p_i^R denotes the average transmit power of the relay node i, $\eta_{i,s}^R$ is the channel noise with $\|\eta_{i,s}^R\|_2 \leq \bar{\eta}_i^R$, and $h_{i,s}^R \sim$

$\mathcal{N}(\bar{h}_i^R, \tilde{h}_i^R)$ is the relay-to-estimator channel parameter. $\eta_{i,s}$ is defined as the overall noise. By applying the triangle inequality and the sub-multiplicative property of the induced ℓ_2-norm, the following bound holds:

$$\|\eta_{i,s}\|_2 \leq \sqrt{p_i^R}\left|h_{i,s}^R\right|\left(\|\Phi_i\|_2\left\|\eta_{i,s}^S\right\|_2+\left\|\eta_{i,s}^C\right\|_2\right)+\|\eta_{i,s}^R\|_2. \tag{7}$$

Since $h_{i,s}^R$ follows a Gaussian distribution, i.e., $h_{i,s}^R \sim \mathcal{N}(\bar{h}_i^R, \tilde{h}_i^R)$, for a prescribed confidence level $0 < \alpha_i^R < 1$, there exists a constant $\beta_i^R > 0$ such that

$$\Pr\left\{\left|h_{i,s}^R-\bar{h}_i^R\right| \leq \beta_i^R\sqrt{\tilde{h}_i^R}\right\}=\alpha_i^R. \tag{8}$$

Consequently, the overall noise $\eta_{i,s}$ satisfies

$$\Pr\left\{\|\eta_{i,s}\|_2 \leq \bar{\eta}_i\right\} \geq \alpha_i^R \tag{9}$$

where

$$\bar{\eta}_i \triangleq \sqrt{p_i^R}\left(|\bar{h}_i^R|+\beta_i^R\sqrt{\tilde{h}_i^R}\right)\left(\|\Phi_i\|_2\,\bar{\eta}_i^S+\bar{\eta}_i^C\right)+\bar{\eta}_i^R.$$

5) Signal reconstruction at estimator: Based on the received signal $z_{i,s}^R$, the estimator reconstructs the signal as follows:

$$\hat{\zeta}_{i,s}=\sqrt{p_i^R p_i^S}\,\bar{h}_i^R\bar{h}_i^S\Psi_i\hat{\mathbf{s}}_{i,s} \tag{10}$$

where $\hat{\mathbf{s}}_{i,s}$ is obtained by solving the following convex optimization problem:

$$\begin{aligned}\hat{\mathbf{s}}_{i,s}^\star &= \arg\min_{\hat{\mathbf{s}}_{i,s}}\|\hat{\mathbf{s}}_{i,s}\|_1\\ \text{s.t.}\ &\left\|z_{i,s}^R-\sqrt{p_i^R p_i^S}\,\bar{h}_i^R\bar{h}_i^S\Phi_i\Psi_i\hat{\mathbf{s}}_{i,s}\right\|_2 \leq \bar{\eta}_i+\bar{\epsilon}_i\end{aligned} \tag{11}$$

where the term $\bar{\epsilon}_i$ characterizes the mismatch caused by the random channel fluctuations.

The effect of random channel fluctuations can be characterized by

$$\|\epsilon_{i,s}\|_2 \leq \sqrt{p_i^R p_i^S}\left|h_{i,s}^R h_{i,s}^S-\bar{h}_i^R\bar{h}_i^S\right|\|\Phi_i\Psi_i\mathbf{s}_{i,s}\|_2\,. \tag{12}$$

Note that the boundedness of the random channel perturbation requires an upper bound on the norm $\|\Psi_i\mathbf{s}_{i,s}\|_2$. Since $y_{i,s}=\Psi_i\mathbf{s}_{i,s}$, this requirement is equivalent to assuming that the sensor measurement $y_{i,s}$ has finite ℓ_2-norm. In practical systems, such a bound is usually available, because it is determined by sensor hardware characteristics and transmission power constraints.

Since $h_{i,s}^S$ is a Gaussian random variables, for a prescribed confidence level $0 < \alpha_i^S < 1$, there exists a constant $\beta_i^S > 0$ such that

$$\Pr\left\{\left|h_{i,s}^S-\bar{h}_i^S\right| \leq \beta_i^S\sqrt{\tilde{h}_i^S}\right\}=\alpha_i^S. \tag{13}$$

By virtue of the mutual independence of $h_{i,s}^R$ and $h_{i,s}^S$, the joint event that both channel parameters lie within their respective confidence intervals occurs with probability no less than $\alpha_i^R\alpha_i^S$. Accordingly, $\epsilon_{i,s}$ admits the following bound:

$$\Pr\left\{\|\epsilon_{i,s}\|_2 \leq \bar{\epsilon}_i\right\} \geq \alpha_i^S\alpha_i^R \tag{14}$$

where

$$\bar{\epsilon}_i \triangleq \sqrt{p_i^R p_i^S}\left(\beta_i^S|\bar{h}_i^R|\sqrt{\tilde{h}_i^S}+\beta_i^R|\bar{h}_i^S|\sqrt{\tilde{h}_i^R}+\beta_i^R\beta_i^S \times\sqrt{\tilde{h}_i^R\tilde{h}_i^S}\right)\|\Phi_i\Psi_i\mathbf{s}_{i,s}\|_2\,.$$

Remark 1: The constraint in the decompression optimization problem is constructed on the basis of high-probability confidence bounds for the random channel parameters $h_{i,s}^S$ and $h_{i,s}^R$. For prescribed confidence levels $0 < \alpha_i^S, \alpha_i^R < 1$, the corresponding confidence intervals are given by $|h_{i,s}^S-\bar{h}_i^S| \leqslant \beta_i^S\sqrt{\tilde{h}_i^S}$ and $|h_{i,s}^R-\bar{h}_i^R| \leqslant \beta_i^R\sqrt{\tilde{h}_i^R}$, where β_i^S and β_i^R are chosen such that $\Pr\{|h_{i,s}^{\cdot}-\bar{h}_i^{\cdot}| \leqslant \beta_i^{\cdot}\sqrt{\tilde{h}_i^{\cdot}}\}=\alpha_i^{\cdot}$ ($\cdot \in \{S,R\}$). Owing to the independence of $h_{i,s}^S$ and $h_{i,s}^R$, the probability that both parameters simultaneously lie within their respective confidence intervals is at least $\alpha_i^S\alpha_i^R$, which provides a lower bound on the feasibility confidence of the reconstruction constraint. For the complementary event, whose probability is no greater than $1-\alpha_i^S\alpha_i^R$, at least one coefficient violates its confidence bound, and the received signal $z_{i,s}^R$ may then be subject to severe channel-induced distortion. Rather than discarding such measurements, the corresponding reconstructed signals are conservatively modeled as an unknown but bounded disturbance. In this way, all received data can be incorporated into the estimation framework, channel distortions can be explicitly taken into account, and the robustness of the subsequent state estimation scheme can be preserved.

Lemma 1 (Reconstruction Error Bound [5]): Let $\hat{\zeta}$ be the reconstructed signal obtained by solving the convex optimization problem (15), ζ_c be the received compression signal, Φ be the compression matrix, and Ψ be the transform domain:

$$\hat{\mathbf{s}}^\star=\arg\min_{\hat{\mathbf{s}}}\|\hat{\mathbf{s}}\|_1 \quad \text{s.t.} \quad \|\zeta_c-\Phi\Psi\hat{\mathbf{s}}\|_2 \leq \bar{\eta} \tag{15}$$

where $\bar{\eta}$ is the noise bound. If Φ satisfies the RIP of order $2K$ with constant $\delta_{2K} < \sqrt{2}-1$, the reconstruction error is bounded as follows:

$$\|\hat{\zeta}-\zeta\|_2 \leq a\frac{\sigma_K(\zeta)_1}{\sqrt{K}}+b\bar{\eta},\ \ \sigma_K(\mathbf{y})_1=\|\mathbf{s}-\mathbf{s}_K\|_1 \tag{16}$$

where $\zeta=\Psi\mathbf{s}$, $\sigma_K(\mathbf{y})_1$ is the K-term best approximation error, $\mathbf{s}_K$ is the best K-term approximation of $\mathbf{s}$, and

$$a=2\frac{1-(1-\sqrt{2})\delta_{2K}}{1-(1+\sqrt{2})\delta_{2K}},\ \ b=4\frac{\sqrt{1+\delta_{2K}}}{1-(1+\sqrt{2})\delta_{2K}}.$$

Lemma 2 (K-Term Approximation Error Bound [7]): Let $\mathbf{s}$, $\mathbf{s}_K$, and $\sigma_K(\mathbf{y})_1$ be defined as in Lemma 1. Assume that the transform domain coefficients of ζ satisfy a compressibility condition: when arranged in non-increasing order of magnitude, denoted by $|s|_{(1)} \geq |s|_{(2)} \geq \cdots \geq |s|_{(n_y)}$, there exist constants $H > 0$ and $\gamma > 1$ such that

$$|s|_{(\kappa)} \leq H\kappa^{-\gamma}, \quad \kappa=1,2,\ldots,n_y.$$

Then, the K-term approximation error admits the following bound:

$$\sigma_K(\zeta)_1 \leq \frac{H}{\gamma-1}K^{1-\gamma} \triangleq \bar{\sigma}_K. \tag{17}$$

In particular, for a fixed sparsity level K, $\sigma_K(\zeta)_1$ is uniformly bounded by a time-invariant constant determined by the signal prior.

According to Lemmas 1 and 2, if Φ_i satisfies the RIP of order $2K$ and $\delta_{2K} < \sqrt{2}-1$, the reconstruction error of the CF relay under the CS techniques can be expressed as follows:

$$\|\hat{\zeta}_{i,s} - \bar{\zeta}_{i,s}\|_2 \leq d_i \tag{18}$$

where

$$\bar{\zeta}_{i,s} \triangleq \sqrt{p_i^S p_i^R}\bar{h}_i^S \bar{h}_i^R \Psi_i \mathbf{s}_{i,s},$$
$$\hat{\zeta}_{i,s} \triangleq \sqrt{p_i^S p_i^R}\bar{h}_i^S \bar{h}_i^R \Psi_i \hat{\mathbf{s}}_{i,s},$$
$$d_i \triangleq a\frac{\bar{\sigma}_K}{\sqrt{K}} + b(\bar{\epsilon}_i + \bar{\eta}_i).$$

Remark 2: From (18), we observe that the reconstruction error consists of three distinct components: the sparsity approximation error, the error introduced by random channel parameters, and the noise effect. Since the random channel parameters only scale the transmitted signal without altering its sparsity structure, they do not affect the sparsity approximation term in Lemma 1. In particular, when the compression process is noiseless (i.e., $\eta_{i,s}^S = \eta_{i,s}^C = \eta_{i,s}^R = 0$), the reconstruction error reduces to the sparsity approximation error and the error induced by random channel parameters. Furthermore, if the signal $y_{i,s}$ is exactly K-sparse in the transform domain (i.e., $\sigma_K(y_i)_1 = \|\mathbf{s} - \mathbf{s}_K\|_1 = 0$), the reconstruction error reduces only to the error caused by the random channel parameters. This demonstrates that with random channel parameters, the CS framework achieves exact recovery for truly K-sparse signals in the absence of measurement noise.

Based on the above analysis, the available signal $\tilde{\zeta}_{i,s}$ at the estimator is modeled by

$$\tilde{\zeta}_{i,s} = \alpha_{i,s}\hat{\zeta}_{i,s} + (1-\alpha_{i,s})\varsigma_{i,s} \tag{19}$$

where $\varsigma_{i,s}$ denotes the reconstruction-failed signal satisfying

$$\|\varsigma_{i,s}\|_2 \leq c_i \tag{20}$$

with c_i being determined by the hardware constraints of the computational unit.

Remark 3: It should be noted that c_i is a positive constant that bounds the ℓ_2-norm of the reconstruction-failed signal. Physically, this bound originates from the hard amplitude limits imposed by the hardware of the sensing and communication system. For a typical resource-constrained sensor node equipped with an n_y-channel analog-to-digital converter with a saturation voltage of $\pm V_{\max}$ per channel, the worst-case ℓ_2-norm bound is given by $c_i = V_{\max}\sqrt{n_y}$, which corresponds to the maximum possible signal energy when all analog-to-digital converter channels are saturated simultaneously. This conservative bound ensures that even in the extreme case of complete CS reconstruction failure, the signal magnitude remains strictly bounded.

The variable $\alpha_{i,s}$ is a Bernoulli-distributed random variable satisfying

$$\text{Prob}\{\alpha_{i,s} = 1\} = \bar{\alpha}_i,$$
$$\text{Prob}\{\alpha_{i,s} = 0\} = 1 - \bar{\alpha}_i \tag{21}$$

where $\bar{\alpha}_i$ denotes the probability of the successful reconstruction and satisfies $\bar{\alpha}_i \geq \alpha_i^R \alpha_i^S$.

Remark 4: This paper considers a CF relay architecture enhanced by the CS techniques. Such an architecture is particularly suitable for WSNs because the physical coverage of the network can be extended, while computationally intensive signal-processing tasks, such as compression, can be shifted from energy-limited and computation-limited sensor nodes to a relay node with more abundant resources. It should also be noted that, owing to random channel fading and noise, the CS recovery process may not always remain feasible. Such inherent uncertainty motivates the probabilistic modeling of the CS-based reconstruction outcome adopted in this paper.

B. Distributed Recursive State Estimation Problem

Let $\hat{x}_{i,s+1|s}$ and $\hat{x}_{i,s+1|s+1}$ be the one-step prediction and the updated state estimate of the i-th node, respectively. The distributed recursive state estimator is designed as follows:

$$\hat{x}_{i,s+1|s} = A_s \hat{x}_{i,s|s}, \tag{22}$$

$$\begin{aligned}\hat{x}_{i,s+1|s+1} &= \hat{x}_{i,s+1|s} + L_{i,s+1}(\tilde{\zeta}_{i,s+1} - C_{i,s+1}^* \bar{\alpha}_i \hat{x}_{i,s+1|s}) \\ &\quad + K_{i,s+1}\sum_{j\in\mathbf{N}_i} a_{ij}\left(\tilde{\zeta}_{j,s+1} - C_{j,s+1}^* \bar{\alpha}_j \hat{x}_{j,s+1|s}\right)\end{aligned} \tag{23}$$

where $C_{i,s+1}^* \triangleq \sqrt{p_i^R p_i^S}\bar{h}_i^R \bar{h}_i^S C_{i,s+1}$, $L_{i,s+1}$ and $K_{i,s+1}$ are the state estimator parameters to be designed.

Define $e_{i,s+1|s} \triangleq x_{s+1} - \hat{x}_{i,s+1|s}$ and $e_{i,s+1|s+1} \triangleq x_{s+1} - \hat{x}_{i,s+1|s+1}$ as the prediction error and the estimation error, respectively. The corresponding covariance matrices are defined as $P_{i,s+1|s} \triangleq \mathbb{E}\{e_{i,s+1|s}e_{i,s+1|s}^T\}$ and $P_{i,s+1|s+1} \triangleq \mathbb{E}\{e_{i,s+1|s+1}e_{i,s+1|s+1}^T\}$.

For a compact network-level analysis, the node-wise estimation errors are augmented into a global error vector. The corresponding prediction and estimation error covariance matrices are denoted by $P_{s+1|s}$ and $P_{s+1|s+1}$, respectively, whose diagonal blocks are given by $P_{i,s+1|s}$ and $P_{i,s+1|s+1}$.

The objectives of this paper are summarized as follows.

1) Derive an upper bound on the estimation error covariance $P_{s+1|s+1}$.
2) Minimize the derived upper bound by appropriately designing the estimator gains $L_{i,s+1}$ and $K_{i,s+1}$ in the distributed estimators (22) and (23).

III. Main Results

In this section, the distributed state estimation scheme is designed by minimizing an upper bound on the estimation error covariance. Before the main results are presented, the following three lemmas are introduced.

Lemma 3: [36] For any two vectors $z, o \in \mathbb{R}^n$, the inequality

$$zo^T + oz^T \leq \varepsilon zz^T + \varepsilon^{-1}oo^T$$

holds with $\varepsilon > 0$ being a constant scalar.

Lemma 4: [27] Let $A=[a_{ij}]_{n\times n}$ be a real valued matrix and $B=\mathrm{diag}\{b_1,b_2,\ldots,b_n\}$ be a diagonal stochastic matrix. The following relationship holds:

$$\mathbb{E}\{BAB^T\}=\begin{bmatrix}\mathbb{E}\{b_1^2\} & \mathbb{E}\{b_1b_2\} & \cdots & \mathbb{E}\{b_1b_n\}\\ \mathbb{E}\{b_2b_1\} & \mathbb{E}\{b_2^2\} & \cdots & \mathbb{E}\{b_2b_n\}\\ \vdots & \vdots & \ddots & \vdots\\ \mathbb{E}\{b_nb_1\} & \mathbb{E}\{b_nb_2\} & \cdots & \mathbb{E}\{b_n^2\}\end{bmatrix}\circ A$$

where $\circ$ is the Hadamard product defined as $[A\circ B]_{ij}=A_{ij}\cdot B_{ij}$.

Lemma 5: [32] For matrices X, Y, Z and symmetric matrix P with appropriate dimensions, the following equalities hold:

$$\frac{\partial\mathrm{tr}(XYZ)}{Y}=X^TZ^T,\ \frac{\partial\mathrm{tr}(XY^TZ)}{Y}=ZX,$$
$$\frac{\partial\mathrm{tr}[(XYZ)P(XYZ)^T]}{Y}=2X^TXYZPZ^T.$$

The state covariance matrix is calculated as follows:

$$X_{s+1}\triangleq\ \mathbb{E}\{x_{s+1}x_{s+1}^T\}=\ A_sX_sA_s^T+B_sQ_sB_s^T.\tag{24}$$

For notational convenience, the following quantities are introduced:

$$\begin{aligned}\mathcal{A}_s&\triangleq I_N\otimes A_s,\ \mathcal{B}_s\triangleq\ I_N\otimes B_s,\ \varsigma_{s+1}\triangleq\mathrm{col_N}\{\varsigma_{i,s+1}\},\\ R_s&\triangleq\mathrm{diag}\{R_{1,s},\ \ldots,\ R_{N,s}\},\ \mathcal{Q}_s\triangleq 1_{N\times N}\otimes Q_s,\\ \mathcal{L}_{s+1}&\triangleq\mathrm{diag}\{L_{1,s+1},\ \ldots,\ L_{N,s+1}\},\ v_{s+1}\triangleq\mathrm{col_N}\{v_{i,s+1}\},\\ \mathcal{K}_{s+1}&\triangleq\mathrm{diag}\{K_{1,s+1},\ \ldots,\ K_{N,s+1}\},\ \bar{\zeta}_{s+1}\triangleq\mathrm{col_N}\{\bar{\zeta}_{i,s+1}\},\\ \mathcal{X}_{s+1}&\triangleq 1_{N\times N}\otimes X_{s+1},\ \bar{\omega}_s\triangleq\mathrm{col_N}\{\omega_s\},\\ \bar{\Lambda}&\triangleq\Lambda\otimes I_{n_y},\ \hat{\zeta}_{s+1}\triangleq\mathrm{col_N}\{\hat{\zeta}_{i,s+1}\},\\ \alpha_{s+1}&\triangleq\mathrm{diag}\{\alpha_{1,s+1}I_{n_y},\ldots,\alpha_{N,s+1}I_{n_y}\},\\ \bar{\alpha}&\triangleq\mathrm{diag}\{\bar{\alpha}_1I_{n_y},\ldots,\bar{\alpha}_NI_{n_y}\},\\ \mathcal{C}_{s+1}^*&\triangleq\mathrm{diag}\{C_{1,s+1}^*,\ \ldots,\ C_{N,s+1}^*\},\\ \mathcal{D}_{s+1}^*&\triangleq\mathrm{diag}\{D_{1,s+1}^*,\ \ldots,\ D_{N,s+1}^*\},\\ c&\triangleq\sqrt{\sum_{i=1}^N(c_i^2)},\ d\triangleq\ \sqrt{\sum_{i=1}^N(d_i^2)}.\end{aligned}$$

Theorem 1: Given positive scalars μ, $\hbar_1$, $\hbar_2$, $\hbar_3$, $\hbar_4$ and $\hbar_5$, for the distributed state estimators (22) and (23), the prediction and estimation error covariances $P_{s+1|s}$ and $P_{s+1|s+1}$ satisfy

$$P_{s+1|s}\leq\Gamma_{s+1|s},$$
$$P_{s+1|s+1}\leq\Gamma_{s+1|s+1},$$

where

$$\begin{aligned}\Gamma_{s+1|s}&\triangleq\mathcal{A}_s\Gamma_{s|s}\mathcal{A}_s^T+\mathcal{B}_s\mathcal{Q}_s\mathcal{B}_s^T,\\ \Gamma_{s+1|s+1}&\triangleq(1+\hbar_1+\hbar_2)\Pi_{1,s+1}\Gamma_{s+1|s}\Pi_{1,s+1}^T\\ &\quad+\mathcal{L}_{s+1}\Lambda_{s+1}^1\mathcal{L}_{s+1}^T+\mathcal{K}_{s+1}\Lambda_{s+1}^2\mathcal{K}_{s+1}^T\\ &\quad+\mathcal{L}_{s+1}\Lambda_{s+1}^3\mathcal{K}_{s+1}^T+\mathcal{K}_{s+1}\Lambda_{s+1}^4\mathcal{L}_{s+1}^T\\ \Lambda_{s+1}^1&\triangleq(1+\hbar_3)(\hat{\alpha}\circ((1+\mu^{-1})d^2I+(1+\mu)(\mathcal{C}_{s+1}^*\\ &\quad\times\mathcal{X}_{s+1}(\mathcal{C}_{s+1}^*)^T+\mathcal{D}_{s+1}^*R_{s+1}(\mathcal{D}_{s+1}^*)^T)))\\ &\quad+(1+\hbar_1^{-1}+\hbar_4+\hbar_5)d^2\bar{\alpha}\bar{\alpha}^T\\ &\quad+(1+\hbar_4^{-1})\bar{\alpha}\mathcal{D}_{s+1}^*R_{s+1}(\mathcal{D}_{s+1}^*)^T\bar{\alpha}^T\\ &\quad+(1+\hbar_2^{-1}+\hbar_3^{-1}+\hbar_5^{-1})(I-\bar{\alpha})c^2,\\ \Lambda_{s+1}^2&\triangleq\bar{\Lambda}\Lambda_{s+1}^1\bar{\Lambda}^T,\ \Lambda_{s+1}^3\triangleq\Lambda_{s+1}^1\bar{\Lambda}^T,\ \Lambda_{s+1}^4\triangleq\bar{\Lambda}\Lambda_{s+1}^1,\\ \hat{\alpha}&\triangleq\mathrm{diag}\{(\bar{\alpha}_1-\bar{\alpha}_1^2)1_{n_y\times n_y},\ldots,(\bar{\alpha}_N-\bar{\alpha}_N^2)1_{n_y\times n_y}\},\\ \Pi_{1,s+1}&\triangleq I-(\mathcal{L}_{s+1}+\mathcal{K}_{s+1}\bar{\Lambda})\bar{\alpha}\mathcal{C}_{s+1}^*.\end{aligned}$$

Proof: Considering (1), (22), and (23), the error dynamics is acquired as follows:

$$e_{i,s+1|s}=A_se_{i,s|s}+B_s\omega_s,\tag{25}$$

$$\begin{aligned}e_{i,s+1|s+1}&=e_{i,s+1|s}-L_{i,s+1}\Big((\alpha_{i,s+1}\hat{\zeta}_{i,s+1}-\bar{\alpha}_i\hat{\zeta}_{i,s+1})\\ &\quad+\bar{\alpha}_i(\hat{\zeta}_{i,s+1}-\bar{\zeta}_{i,s+1})+\bar{\alpha}_i(\bar{\zeta}_{i,s+1}\\ &\quad-C_{i,s+1}^*\hat{x}_{i,s+1|s})+(1-\alpha_{i,s+1})\varsigma_{i,s+1}\Big)\\ &\quad-K_{i,s+1}\sum_{j\in\mathbf{N}_i}a_{ij}\Big((\alpha_{j,s+1}\hat{\zeta}_{j,s+1}\\ &\quad-\bar{\alpha}_j\hat{\zeta}_{j,s+1})+\bar{\alpha}_j(\hat{\zeta}_{j,s+1}-\bar{\zeta}_{j,s+1})\\ &\quad+\bar{\alpha}_j(\bar{\zeta}_{j,s+1}-C_{j,s+1}^*\hat{x}_{j,s+1|s})\\ &\quad+(1-\alpha_{j,s+1})\varsigma_{j,s+1}\Big)\\ &=e_{i,s+1|s}-L_{i,s+1}\Big((\alpha_{i,s+1}-\bar{\alpha}_i)\hat{\zeta}_{i,s+1}\\ &\quad+\bar{\alpha}_i(\hat{\zeta}_{i,s+1}-\bar{\zeta}_{i,s+1})+\bar{\alpha}_i(C_{i,s+1}^*e_{i,s+1|s}\\ &\quad+D_{i,s+1}^*v_{i,s+1})+(1-\alpha_{i,s+1})\varsigma_{i,s+1}\Big)\\ &\quad-K_{i,s+1}\sum_{j\in\mathbf{N}_i}a_{ij}\Big((\alpha_{j,s+1}-\bar{\alpha}_j)\hat{\zeta}_{j,s+1}\\ &\quad+\bar{\alpha}_j(\hat{\zeta}_{j,s+1}-\bar{\zeta}_{j,s+1})+\bar{\alpha}_j(C_{j,s+1}^*e_{j,s+1|s}\\ &\quad+D_{j,s+1}^*v_{j,s+1})+(1-\alpha_{j,s+1})\varsigma_{j,s+1}\Big)\end{aligned}\tag{26}$$

where $D_{i,s+1}^*\triangleq\sqrt{p_i^Rp_i^S}\bar{h}_i^R\bar{h}_i^SD_{i,s+1}$.

The compact forms of (25) and (26) are, respectively, obtained as follows:

$$e_{s+1|s}=\mathcal{A}_se_{s|s}+\mathcal{B}_s\bar{\omega}_s,\tag{27}$$

$$\begin{aligned}e_{s+1|s+1}&=e_{s+1|s}-\mathcal{L}_{s+1}\big((\alpha_{s+1}-\bar{\alpha})\hat{\zeta}_{s+1}\\ &\quad+\bar{\alpha}(\hat{\zeta}_{s+1}-\bar{\zeta}_{s+1})+\bar{\alpha}(\mathcal{C}_{s+1}^*e_{s+1|s}+\mathcal{D}_{s+1}^*v_{s+1})\\ &\quad+(I-\alpha_{s+1})\varsigma_{s+1}\big)-\mathcal{K}_{s+1}\bar{\Lambda}\big((\alpha_{s+1}-\bar{\alpha})\hat{\zeta}_{s+1}\\ &\quad+\bar{\alpha}(\hat{\zeta}_{s+1}-\bar{\zeta}_{s+1})+\bar{\alpha}(\mathcal{C}_{s+1}^*e_{s+1|s}+\mathcal{D}_{s+1}^*v_{s+1})\\ &\quad+(I-\alpha_{s+1})\varsigma_{s+1}\big)\\ &=\Pi_{1,s+1}e_{s+1|s}+\Pi_{2,s+1}\hat{\zeta}_{s+1}+\Pi_{4,s+1}v_{s+1}\\ &\quad+\Pi_{3,s+1}(\hat{\zeta}_{s+1}-\bar{\zeta}_{s+1})+\Pi_{5,s+1}\varsigma_{s+1}\end{aligned}\tag{28}$$

where

$$\begin{aligned}\Pi_{2,s+1}&\triangleq-(\mathcal{L}_{s+1}+\mathcal{K}_{s+1}\bar{\Lambda})(\alpha_{s+1}-\bar{\alpha}),\\ \Pi_{3,s+1}&\triangleq-(\mathcal{L}_{s+1}+\mathcal{K}_{s+1}\bar{\Lambda})\bar{\alpha},\\ \Pi_{4,s+1}&\triangleq-(\mathcal{L}_{s+1}+\mathcal{K}_{s+1}\bar{\Lambda})\bar{\alpha}\mathcal{D}_{s+1}^*,\\ \Pi_{5,s+1}&\triangleq-(\mathcal{L}_{s+1}+\mathcal{K}_{s+1}\bar{\Lambda})(I-\alpha_{s+1}).\end{aligned}$$

The prediction error covariance $P_{s+1|s}$ is expressed by

$$P_{s+1|s} = \mathcal{A}_s P_{s|s} \mathcal{A}_s^T + \mathcal{B}_s \mathcal{Q}_s \mathcal{B}_s^T. \tag{29}$$

The estimation error covariance $P_{s+1|s+1}$ is calculated as follows:

$$\begin{aligned}
& P_{s+1|s+1} \\
&= \mathbb{E}\Big\{\Pi_{1,s+1}e_{s+1|s}e_{s+1|s}^T\Pi_{1,s+1}^T + \Pi_{2,s+1}\hat{\zeta}_{s+1}\hat{\zeta}_{s+1}^T\Pi_{2,s+1}^T \\
&\quad + \Pi_{3,s+1}(\hat{\zeta}_{s+1}-\bar{\zeta}_{s+1})(\hat{\zeta}_{s+1}-\bar{\zeta}_{s+1})^T\Pi_{3,s+1}^T \\
&\quad + \Pi_{4,s+1}v_{s+1}v_{s+1}^T\Pi_{4,s+1}^T + \Pi_{5,s+1}\varsigma_{s+1}\varsigma_{s+1}^T\Pi_{5,s+1}^T \\
&\quad + \Pi_{1,s+1}e_{s+1|s}\hat{\zeta}_{s+1}^T\Pi_{2,s+1}^T + \Pi_{2,s+1}\hat{\zeta}_{s+1}e_{s+1|s}^T\Pi_{1,s+1}^T \\
&\quad + \Pi_{1,s+1}e_{s+1|s}(\hat{\zeta}_{s+1}-\bar{\zeta}_{s+1})^T\Pi_{3,s+1}^T \\
&\quad + \Pi_{3,s+1}(\hat{\zeta}_{s+1}-\bar{\zeta}_{s+1})e_{s+1|s}^T\Pi_{1,s+1}^T \\
&\quad + \Pi_{1,s+1}e_{s+1|s}v_{s+1}^T\Pi_{4,s+1}^T + \Pi_{4,s+1}v_{s+1}e_{s+1|s}^T\Pi_{1,s+1}^T \\
&\quad + \Pi_{1,s+1}e_{s+1|s}\varsigma_{s+1}^T\Pi_{5,s+1}^T + \Pi_{5,s+1}\varsigma_{s+1}e_{s+1|s}^T\Pi_{1,s+1}^T \\
&\quad + \Pi_{2,s+1}\hat{\zeta}_{s+1}(\hat{\zeta}_{s+1}-\bar{\zeta}_{s+1})^T\Pi_{3,s+1}^T \\
&\quad + \Pi_{3,s+1}(\hat{\zeta}_{s+1}-\bar{\zeta}_{s+1})\hat{\zeta}_{s+1}^T\Pi_{2,s+1}^T \\
&\quad + \Pi_{2,s+1}\hat{\zeta}_{s+1}v_{s+1}^T\Pi_{4,s+1}^T + \Pi_{4,s+1}v_{s+1}\hat{\zeta}_{s+1}^T\Pi_{2,s+1}^T \\
&\quad + \Pi_{2,s+1}\hat{\zeta}_{s+1}\varsigma_{s+1}^T\Pi_{5,s+1}^T + \Pi_{5,s+1}\varsigma_{s+1}\hat{\zeta}_{s+1}^T\Pi_{2,s+1}^T \\
&\quad + \Pi_{3,s+1}(\hat{\zeta}_{s+1}-\bar{\zeta}_{s+1})v_{s+1}^T\Pi_{4,s+1}^T \\
&\quad + \Pi_{4,s+1}v_{s+1}(\hat{\zeta}_{s+1}-\bar{\zeta}_{s+1})^T\Pi_{3,s+1}^T \\
&\quad + \Pi_{3,s+1}(\hat{\zeta}_{s+1}-\bar{\zeta}_{s+1})\varsigma_{s+1}^T\Pi_{5,s+1}^T \\
&\quad + \Pi_{5,s+1}\varsigma_{s+1}(\hat{\zeta}_{s+1}-\bar{\zeta}_{s+1})^T\Pi_{3,s+1}^T \\
&\quad + \Pi_{4,s+1}v_{s+1}\varsigma_{s+1}^T\Pi_{5,s+1}^T + \Pi_{5,s+1}\varsigma_{s+1}v_{s+1}^T\Pi_{4,s+1}^T\Big\} \\
&= \mathbb{E}\Big\{\Pi_{1,s+1}e_{s+1|s}e_{s+1|s}^T\Pi_{1,s+1}^T + \Pi_{2,s+1}\hat{\zeta}_{s+1}\hat{\zeta}_{s+1}^T\Pi_{2,s+1}^T \\
&\quad + \Pi_{3,s+1}(\hat{\zeta}_{s+1}-\bar{\zeta}_{s+1})(\hat{\zeta}_{s+1}-\bar{\zeta}_{s+1})^T\Pi_{3,s+1}^T \\
&\quad + \Pi_{4,s+1}v_{s+1}v_{s+1}^T\Pi_{4,s+1}^T + \Pi_{5,s+1}\varsigma_{s+1}\varsigma_{s+1}^T\Pi_{5,s+1}^T \\
&\quad + \Pi_{1,s+1}e_{s+1|s}(\hat{\zeta}_{s+1}-\bar{\zeta}_{s+1})^T\Pi_{3,s+1}^T \\
&\quad + \Pi_{3,s+1}(\hat{\zeta}_{s+1}-\bar{\zeta}_{s+1})e_{s+1|s}^T\Pi_{1,s+1}^T \\
&\quad + \Pi_{1,s+1}e_{s+1|s}\varsigma_{s+1}^T\Pi_{5,s+1}^T + \Pi_{5,s+1}\varsigma_{s+1}e_{s+1|s}^T\Pi_{1,s+1}^T \\
&\quad + \Pi_{2,s+1}\hat{\zeta}_{s+1}\varsigma_{s+1}^T\Pi_{5,s+1}^T + \Pi_{5,s+1}\varsigma_{s+1}\hat{\zeta}_{s+1}^T\Pi_{2,s+1}^T \\
&\quad + \Pi_{3,s+1}(\hat{\zeta}_{s+1}-\bar{\zeta}_{s+1})v_{s+1}^T\Pi_{4,s+1}^T \\
&\quad + \Pi_{4,s+1}v_{s+1}(\hat{\zeta}_{s+1}-\bar{\zeta}_{s+1})^T\Pi_{3,s+1}^T \\
&\quad + \Pi_{3,s+1}(\hat{\zeta}_{s+1}-\bar{\zeta}_{s+1})\varsigma_{s+1}^T\Pi_{5,s+1}^T \\
&\quad + \Pi_{5,s+1}\varsigma_{s+1}(\hat{\zeta}_{s+1}-\bar{\zeta}_{s+1})^T\Pi_{3,s+1}^T\Big\}.
\end{aligned} \tag{30}$$

It follows from (18) and (24) that

$$\begin{aligned}
& \mathbb{E}\{\hat{\zeta}_{s+1}\hat{\zeta}_{s+1}^T\} \\
&= \mathbb{E}\left\{\left(\bar{\zeta}_{s+1} + (\hat{\zeta}_{s+1}-\bar{\zeta}_{s+1})\right)\left(\bar{\zeta}_{s+1} + (\hat{\zeta}_{s+1}-\bar{\zeta}_{s+1})\right)^T\right\} \\
&\le \mathbb{E}\{(1+\mu)\bar{\zeta}_{s+1}\bar{\zeta}_{s+1}^T + (1+\mu^{-1})(\hat{\zeta}_{s+1}-\bar{\zeta}_{s+1}) \\
&\qquad \times (\hat{\zeta}_{s+1}-\bar{\zeta}_{s+1})^T\} \\
&\le \mathbb{E}\{(1+\mu)\bar{\zeta}_{s+1}\bar{\zeta}_{s+1}^T + (1+\mu^{-1})d^2 I\} \\
&= (1+\mu)(\mathcal{C}_{s+1}^*\mathcal{X}_{s+1}(\mathcal{C}_{s+1}^*)^T + \mathcal{D}_{s+1}^* R_{s+1}(\mathcal{D}_{s+1}^*)^T) \\
&\qquad + (1+\mu^{-1})d^2 I.
\end{aligned} \tag{31}$$

According to (29)–(31), Lemma 3, and Lemma 4, one has

$$\begin{aligned}
& P_{s+1|s+1} \\
&\le \mathbb{E}\Big\{(1+\hbar_1+\hbar_2)\Pi_{1,s+1}e_{s+1|s}e_{s+1|s}^T\Pi_{1,s+1}^T + (1+\hbar_3) \\
&\quad \times \Pi_{2,s+1}\hat{\zeta}_{s+1}\hat{\zeta}_{s+1}^T\Pi_{2,s+1}^T + (1+\hbar_1^{-1}+\hbar_4+\hbar_5)\Pi_{3,s+1} \\
&\quad \times d^2 I\Pi_{3,s+1}^T + (1+\hbar_4^{-1})\Pi_{4,s+1}R_{s+1}\Pi_{4,s+1}^T \\
&\quad + (1+\hbar_2^{-1}+\hbar_3^{-1}+\hbar_5^{-1})\Pi_{5,s+1}c^2 I\Pi_{5,s+1}^T\Big\} \\
&= (1+\hbar_1+\hbar_2)\Pi_{1,s+1}P_{s+1|s}\Pi_{1,s+1}^T + \mathcal{L}_{s+1}\Lambda_{s+1}^1\mathcal{L}_{s+1}^T \\
&\quad + \mathcal{K}_{s+1}\Lambda_{s+1}^2\mathcal{K}_{s+1}^T + \mathcal{L}_{s+1}\Lambda_{s+1}^3\mathcal{K}_{s+1}^T + \mathcal{K}_{s+1}\Lambda_{s+1}^4\mathcal{L}_{s+1}^T.
\end{aligned} \tag{32}$$

Following a similar line to that in [36], it can be readily verified that $P_{s+1|s} \le \Gamma_{s+1|s}$ and $P_{s+1|s+1} \le \Gamma_{s+1|s+1}$. The proof is now complete. ■

Remark 5: In this section, the scalars μ and $\hbar_i$, $i = 1, \dots, 5$ are introduced through Young's inequality (Lemma 3) to decouple the cross-covariance terms in the derivation of the estimation error covariance upper bound. Consequently, the resulting bound $\Gamma_{s+1|s+1}$ depends explicitly on these parameters, making their selection an important issue for tightening the bound. While any positive values of μ and $\hbar_i$ are sufficient to guarantee a valid upper bound and the stability of the estimator, obtaining a tighter bound naturally leads to the optimization problem $\min_{\mu,\hbar_i} \operatorname{tr}(\Gamma_{s+1|s+1})$. This problem is generally non-convex. For a more flexible design, one may treat the scalars as time-varying, and then employ evolutionary computation methods (e.g., particle swarm optimization) to search for near-optimal parameters. These techniques are well-suited to handle the non-convexity and can find suitable parameters that yield a nearly optimal upper bound for the estimation error covariance upper bound.

The following theorem is established to design the gain matrices $L_{i,s+1}$ and $K_{i,s+1}$ for the proposed estimators (22) and (23).

Theorem 2: Given positive scalars μ, $\hbar_1$, $\hbar_2$, $\hbar_3$, $\hbar_4$ and $\hbar_5$, for the distributed state estimators (22) and (23), the estimator gain matrices $L_{i,s+1}$ and $K_{i,s+1}$ are designed as follows:

$$\begin{aligned}
L_{i,s+1} &= \left(S_{i,s+1}^1 - \frac{1}{2}\bar{S}_{i,s+1}^2\right)\Xi_{1,s+1}^{-1}, \\
K_{i,s+1} &= \left(S_{i,s+1}^2 - \frac{1}{2}\bar{S}_{i,s+1}^1\right)\Xi_{2,s+1}^{-1}
\end{aligned} \tag{33}$$

where

$$\begin{aligned}
\Omega_{1,i} &\triangleq [\underbrace{0\ 0\ \cdots\ 0}_{i-1} I_{n_x\times n_x} \underbrace{0\ 0\ \cdots\ 0}_{N-i}], \\
\Omega_{2,i} &\triangleq [\underbrace{0\ 0\ \cdots\ 0}_{i-1} I_{n_y\times n_y} \underbrace{0\ 0\ \cdots\ 0}_{N-i}], \\
S_{i,s+1}^1 &\triangleq 2(1+\hbar_1+\hbar_2)\Omega_{1,i}\Gamma_{s+1|s}(\mathcal{C}_{s+1}^*)^T\bar{\alpha}^T\Omega_{2,i}^T, \\
S_{i,s+1}^2 &\triangleq 2(1+\hbar_1+\hbar_2)\Omega_{1,i}\Gamma_{s+1|s}(\mathcal{C}_{s+1}^*)^T\bar{\alpha}^T\bar{\Lambda}^T\Omega_{2,i}^T, \\
\bar{S}_{i,s+1}^1 &\triangleq S_{i,s+1}^1\bar{\Theta}_{1,s+1}^{-1}\left(\bar{\Theta}_{3,s+1} + \bar{\Theta}_{4,s+1}^T\right), \\
\bar{S}_{i,s+1}^2 &\triangleq S_{i,s+1}^2\bar{\Theta}_{2,s+1}^{-1}\left(\bar{\Theta}_{3,s+1}^T + \bar{\Theta}_{4,s+1}\right), \\
\Theta_{1,s+1} &\triangleq (1+\hbar_1+\hbar_2)\bar{\alpha}\mathcal{C}_{s+1}^*\Gamma_{s+1|s}(\mathcal{C}_{s+1}^*)^T\bar{\alpha}^T + \Lambda_{s+1}^1,
\end{aligned}$$

$$
\begin{aligned}
\Theta_{2,s+1} &\triangleq (1+\hbar_1+\hbar_2)\bar{\Lambda}\bar{\alpha}\mathcal{C}^*_{s+1}\Gamma_{s+1|s}(\mathcal{C}^*_{s+1})^T\bar{\alpha}^T \\
&\quad \times \bar{\Lambda}^T + \Lambda^2_{s+1}, \\
\Theta_{3,s+1} &\triangleq (1+\hbar_1+\hbar_2)\bar{\alpha}\mathcal{C}^*_{s+1}\Gamma_{s+1|s}(\mathcal{C}^*_{s+1})^T\bar{\alpha}^T \\
&\quad \times \bar{\Lambda}^T + \Lambda^3_{s+1}, \\
\Theta_{4,s+1} &\triangleq (1+\hbar_1+\hbar_2)\bar{\Lambda}\bar{\alpha}\mathcal{C}^*_{s+1}\Gamma_{s+1|s}(\mathcal{C}^*_{s+1})^T\bar{\alpha}^T \\
&\quad + \Lambda^4_{s+1}, \\
\bar{\Theta}_{1,s+1} &\triangleq \Omega_{2,i}\Theta_{1,s+1}\Omega^T_{2,i}, \quad \bar{\Theta}_{2,s+1} \triangleq \Omega_{2,i}\Theta_{2,s+1}\Omega^T_{2,i}, \\
\bar{\Theta}_{3,s+1} &\triangleq \Omega_{2,i}\Theta_{3,s+1}\Omega^T_{2,i}, \quad \bar{\Theta}_{4,s+1} \triangleq \Omega_{2,i}\Theta_{4,s+1}\Omega^T_{2,i}, \\
\Xi_{1,s+1} &\triangleq 2\bar{\Theta}_{1,s+1} - \frac{1}{2}\left(\bar{\Theta}_{3,s+1}+\bar{\Theta}^T_{4,s+1}\right)\bar{\Theta}^{-1}_{2,s+1} \\
&\quad \times \left(\bar{\Theta}^T_{3,s+1}+\bar{\Theta}_{4,s+1}\right), \\
\Xi_{2,s+1} &\triangleq 2\bar{\Theta}_{2,s+1} - \frac{1}{2}\left(\bar{\Theta}^T_{3,s+1}+\bar{\Theta}_{4,s+1}\right)\bar{\Theta}^{-1}_{1,s+1} \\
&\quad \times \left(\bar{\Theta}_{3,s+1}+\bar{\Theta}^T_{4,s+1}\right).
\end{aligned}
$$

Proof: To facilitate the derivation, we first express the aggregated gain matrices $\mathcal{L}_{s+1}$ and $\mathcal{K}_{s+1}$ in the form of local parameters and projection matrices:

$$
\mathcal{L}_{s+1} = \sum_{i=1}^{N}\Omega^T_{1,i}L_{i,s+1}\Omega_{2,i}, \ \mathcal{K}_{s+1} = \sum_{i=1}^{N}\Omega^T_{1,i}K_{i,s+1}\Omega_{2,i} \tag{34}
$$

where $\Omega_{1,i}$ and $\Omega_{2,i}$ are defined in (33).

The expression of $\Gamma_{s+1|s+1}$ is rewritten as follows:

$$
\begin{aligned}
&\Gamma_{s+1|s+1} \\
&= (1+\hbar_1+\hbar_2)\bigg(\Gamma_{s+1|s} - \left(\mathcal{L}_{s+1}+\mathcal{K}_{s+1}\bar{\Lambda}\right)\bar{\alpha} \\
&\quad \times \mathcal{C}^*_{s+1}\Gamma_{s+1|s} - \Gamma_{s+1|s}(\mathcal{C}^*_{s+1})^T\bar{\alpha}^T\left(\mathcal{L}_{s+1}+\mathcal{K}_{s+1}\bar{\Lambda}\right)^T\bigg) \\
&\quad + \mathcal{L}_{s+1}\Theta_{1,s+1}\mathcal{L}^T_{s+1} + \mathcal{K}_{s+1}\Theta_{2,s+1}\mathcal{K}^T_{s+1} \\
&\quad + \mathcal{L}_{s+1}\Theta_{3,s+1}\mathcal{K}^T_{s+1} + \mathcal{K}_{s+1}\Theta_{4,s+1}\mathcal{L}^T_{s+1}
\end{aligned} \tag{35}
$$

where $\Theta_{1,s+1}$, $\Theta_{2,s+1}$, $\Theta_{3,s+1}$, and $\Theta_{4,s+1}$ are defined in (33).

Substituting (34) into (35) yields

$$
\begin{aligned}
&\mathrm{tr}\left\{\Gamma_{s+1|s+1}\right\} \\
&= \mathrm{tr}\bigg[(1+\hbar_1+\hbar_2)\Gamma_{s+1|s} - (1+\hbar_1+\hbar_2) \\
&\quad \times \bigg(\sum_{i=1}^{N}\Omega^T_{1,i}L_{i,s+1}\Omega_{2,i}\bar{\alpha}\mathcal{C}^*_{s+1}\Gamma_{s+1|s} + \sum_{i=1}^{N}\Omega^T_{1,i}K_{i,s+1} \\
&\quad \times \Omega_{2,i}\bar{\Lambda}\bar{\alpha}\mathcal{C}^*_{s+1}\Gamma_{s+1|s} + \sum_{i=1}^{N}\Gamma_{s+1|s}(\mathcal{C}^*_{s+1})^T\bar{\alpha}^T \\
&\quad \times \Omega^T_{2,i}L^T_{i,s+1}\Omega_{1,i} + \sum_{i=1}^{N}\Gamma_{s+1|s}(\mathcal{C}^*_{s+1})^T\bar{\alpha}^T\bar{\Lambda}^T\Omega^T_{2,i} \\
&\quad \times K^T_{i,s+1}\Omega_{1,i}\bigg) + \sum_{i=1}^{N}\Omega^T_{1,i}L_{i,s+1}\Omega_{2,i}\Theta_{1,s+1}\Omega^T_{2,i}L^T_{i,s+1}\Omega_{1,i} \\
&\quad + \sum_{i=1}^{N}\Omega^T_{1,i}K_{i,s+1}\Omega_{2,i}\Theta_{2,s+1}\Omega^T_{2,i}K^T_{i,s+1}\Omega_{1,i} \\
&\quad + \sum_{i=1}^{N}\Omega^T_{1,i}L_{i,s+1}\Omega_{2,i}\Theta_{3,s+1}\Omega^T_{2,i}K^T_{i,s+1}\Omega_{1,i} \\
&\quad + \sum_{i=1}^{N}\Omega^T_{1,i}K_{i,s+1}\Omega_{2,i}\Theta_{4,s+1}\Omega^T_{2,i}L^T_{i,s+1}\Omega_{1,i}\bigg].
\end{aligned} \tag{36}
$$

Based on the definitions of $\Omega_{1,i}$ and $\Omega_{2,i}$ in (33), the following properties hold:

$$
\begin{aligned}
&\Omega_{1,i}\Omega^T_{1,j} = 0, \ \Omega_{2,i}\Omega^T_{2,j} = 0, \ \text{for } i \neq j, \\
&\Omega_{1,i}\Omega^T_{1,i} = I_{n_x\times n_x}, \ \Omega_{2,i}\Omega^T_{2,i} = I_{n_y\times n_y}.
\end{aligned}
$$

According to Lemma 5, taking the partial derivative of the trace of $\Gamma_{s+1|s+1}$ with respect to $L_{i,s+1}$ and $K_{i,s+1}$, respectively, and letting the derivative be zero, one has

$$
\begin{aligned}
&\frac{\partial \mathrm{tr}(\Gamma_{s+1|s+1})}{\partial L_{i,s+1}} = 0 \\
&\Longrightarrow -S^1_{i,s+1} + 2L_{i,s+1}\bar{\Theta}_{1,s+1} + K_{i,s+1}\left(\bar{\Theta}^T_{3,s+1}+\bar{\Theta}_{4,s+1}\right) \\
&\quad = 0
\end{aligned} \tag{37}
$$

and

$$
\begin{aligned}
&\frac{\partial \mathrm{tr}(\Gamma_{s+1|s+1})}{\partial K_{i,s+1}} = 0 \\
&\Longrightarrow -S^2_{i,s+1} + 2K_{i,s+1}\bar{\Theta}_{2,s+1} + L_{i,s+1}\left(\bar{\Theta}_{3,s+1}+\bar{\Theta}^T_{4,s+1}\right) \\
&\quad = 0.
\end{aligned} \tag{38}
$$

Obviously, $L_{i,s+1}$ and $K_{i,s+1}$ can be determined by solving (37) and (38) simultaneously. The proof is now complete. ■

Remark 6: Compared with distributed estimation schemes employing conventional relay strategies, the proposed CS-CF scheme achieves a favorable trade-off between complexity and performance. Amplify-and-forward relay simply amplifies the received signal with a linear operation, yielding the lowest complexity of $O(n_y)$, but it amplifies channel noise. The decode-and-forward relay performs full decoding and re-encoding, which is generally an NP-hard problem [17]. Consequently, algorithms for this problem typically exhibit exponential computational complexity in the worst case. CF relay lies between amplify-and-forward and decode-and-forward in terms of complexity, as it compresses the signal without complete decoding. In contrast, the proposed CS-CF relay avoids decoding entirely: by leveraging CS technology, it compresses the received signal via a single lightweight matrix-vector multiplication with complexity $O(n_\Phi n_y)$ (where $n_\Phi \ll n_y$). This design avoids the heavy decoding burden of decode-and-forward and the noise amplification of amplify-and-forward, which is particularly beneficial for resource-constrained WSNs.

Remark 7: In this paper, an error model is established by analyzing the impact of random channel fading and channel noise on the decompression error within the CS recovery framework, based on which a distributed recursive state estimator is designed. The main features of the proposed method are summarized as follows:

1) For the first time, the CF relay is systematically introduced into the state estimation problem for WSNs, where CS techniques are employed in place of conventional compression methods. Compared with traditional schemes, the proposed framework exploits CS to significantly reduce both the data volume required for

transmission and the sampling rate while preserving the estimation performance.
2) To the best of the authors' knowledge, this paper represents the first attempt to investigate the impact mechanism of random channel fading on the CS recovery error. By exploiting the statistical characteristics of the channel, a corresponding error model is established, and a state estimator capable of guaranteeing system performance is designed.
3) By taking into account the reconstruction error induced by CS techniques and wireless channel random fading, an upper bound on the estimation error of the proposed estimator is derived, and the estimator parameters are obtained by minimizing this upper bound. The practical effectiveness of the proposed approach will be further validated through a simulation case study based on a USV-MADPS in the following section.

IV. An Illustrative Example

A. Modeling of the MADPS Under Ice-Induced Loads

USVs operating in ice-prone offshore environments are required to maintain precise positioning despite persistent ice loads and environmental disturbances and communication limitations [12], [13], [18]. In such scenarios, ice-induced forces (including extrusion, bending, and sliding loads), wind, waves, and ocean currents introduce continuous external perturbations [2], [25]. Meanwhile, underwater acoustic channels impose severe bandwidth constraints and signal attenuation, which degrade the reliability of state estimation and information transmission in networked USV systems.

To validate the proposed distributed recursive state estimation framework integrating CF relay and CS techniques, an MADPS of a USV operating in ice-prone environments is adopted as the simulation platform. Although a USV is inherently a six-degree-of-freedom system, dynamic positioning performance in ice zones is primarily dominated by heading regulation. Therefore, only the yaw-axis dynamics are considered, while other motions are neglected for simplicity. This modeling choice yields a representative linear system for estimation performance evaluation.

As illustrated in Fig. 2, two reference frames are defined: 1) a body-fixed frame attached to the USV's center of gravity, and 2) an earth-fixed frame following the East-North-Down convention.

The yaw-axis dynamics are described by [29]:

$$\mathcal{M}_{33}\dot{\nu}_3 + \mathcal{N}_{33}\nu_3 + \mathcal{F}_{33}\varrho_3 = \tau_3 + b_{\text{ice}} + d_\omega \tag{39}$$

where ν_3 and ϱ_3 denote the yaw angular velocity and yaw angle, respectively. τ_3 is the yaw control input. b_{ice} represents the slowly varying ice load torque. d_ω denotes the environmental noise. $\mathcal{M}_{33}$, $\mathcal{N}_{33}$ and $\mathcal{F}_{33}$ are the yaw moment of inertia, the yaw hydrodynamic damping coefficient and the tension, respectively.

To capture the slow variation of ice-induced disturbances, b_{ice} is modeled as a first-order inertial system:

$$\dot{b}_{\text{ice}} = -\frac{1}{T_{\text{ice}}} b_{\text{ice}} + d_{\text{ice}} \tag{40}$$

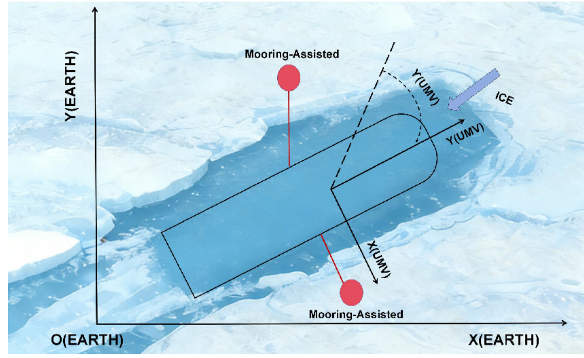

Fig. 2: Body-fixed and earth-fixed reference frames for ice zone USV.

where $T_{\text{ice}} = 50 \sim 100$ is the time constant and d_{ice} represents the stochastic fluctuation noise.

Define the state vector as $x_s \triangleq [\varrho_3^T \ \nu_3^T \ b_{\text{ice}}^T]^T$. Combining (39) and (40), the discrete-time linear state space model employed in the simulation is then given by

$$x_{s+1} = Ax_s + B\tau_3 + E\omega_s \tag{41}$$

where the constant matrices (strictly linear, state-independent) are:

$$A = \begin{bmatrix} 0 & 1 & 0 \\ -\frac{\mathcal{F}_{33}}{\mathcal{M}_{33}} & -\frac{\mathcal{N}_{33}}{\mathcal{M}_{33}} & \frac{1}{\mathcal{M}_{33}} \\ 0 & 0 & -\frac{1}{T_{\text{ice}}} \end{bmatrix} + I, \ \omega_s = \begin{bmatrix} d_\omega \\ d_{\text{ice}} \end{bmatrix},$$

$$B = \begin{bmatrix} 0 \\ \frac{1}{\mathcal{M}_{33}} \\ 0 \end{bmatrix}, \quad E = \begin{bmatrix} 0 & 0 \\ \frac{1}{\mathcal{M}_{33}} & 0 \\ 0 & 1 \end{bmatrix}.$$

In the simulations, the system parameters are chosen as follows [29]:

$$\mathcal{M}_{33} = 2.153, \ \mathcal{N}_{33} = 0.034, \ \mathcal{F}_{33} = 0.651, \ T_{\text{ice}} = 50.$$

B. Simulation Results and Discussion

The effectiveness of the proposed distributed state estimation framework integrating CF relay and CS techniques is evaluated through a series of simulations based on the USV-MADPS model. The estimation performance of the proposed distributed state estimation is examined. Fig. 3 depicts the estimation error trajectories of the first state component obtained by four sensor nodes. To further quantify the estimation accuracy, the mean square error (MSE) is defined as: MSE $\triangleq \frac{1}{N \times n_x}\sum_{\iota=1}^{N\times n_x} \|e_{s|s}^{(\iota)}\|_2^2$. Fig. 4 shows the trace of the minimal upper bound on the estimation error covariance (TMEE) and the MSE of the system, which further validates the effectiveness of the proposed algorithm.

Fig. 5 compares the time-domain trajectories of $\bar{\zeta}1, s$ and $\hat{\zeta}1, s$. Despite the presence of multiplicative channel fading and additive noise, the estimated signal closely follows the true trajectory with bounded deviations, indicating that the proposed framework achieves stable and reliable signal recovery over time. To provide further insight into the underlying CS mechanism. Fig. 6 illustrates the sparse representations of s_1 and $\hat{s}_1$ in the transform domain at a time instant. It can be observed that most coefficients remain close to zero, while the dominant nonzero components are largely preserved in terms of their support. Although certain amplitude deviations are present due to channel fading and noise, the overall sparse structure is effectively recovered, which supports the feasibility of CS-based information recovery in the proposed framework. In addition, Fig. 7 presents the amplitude distribution of the compressed measurement signal z_1^C at the same time in Fig. 6. This signal is obtained by projecting the signal onto a low-dimensional space via the sensing matrix and CF relay transmission, and it exhibits distinct amplitude fluctuations despite interference from channel coefficients and Gaussian noise. This indicates that the core information of the original signal has been effectively encoded in the low-dimensional measurements. Fig. 8 compares the dimension of the signal before compression with the dimension of the signal after compression by the proposed CS-based CF relay. The results show that the proposed framework reduces the required transmission signal dimension by approximately 66%, significantly alleviating the bandwidth burden and energy consumption.

Overall, the above simulation results demonstrate that the proposed distributed estimation framework achieves reliable estimation performance while substantially reducing communication overhead. These results collectively validate the effectiveness of integrating CF relay and CS techniques for state estimation in WSNs.

V. Conclusions

In this paper, the distributed recursive state estimation problem has been addressed for WSNs under stringent resource constraints. An estimation framework integrating CF relay with CS techniques has been proposed. To cope with the

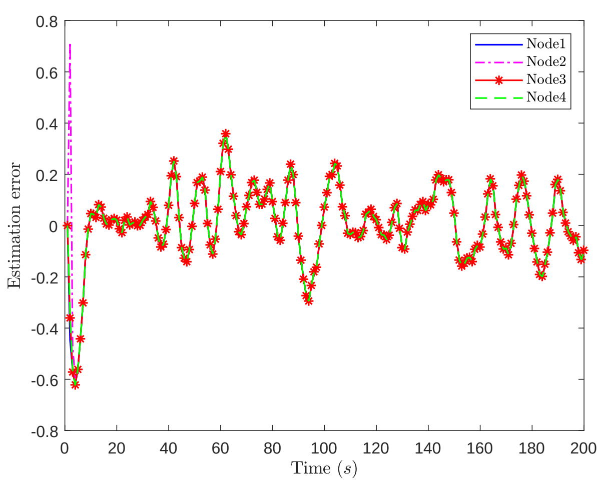

Fig. 3: Estimation error trajectories of the first state component from four sensor nodes.

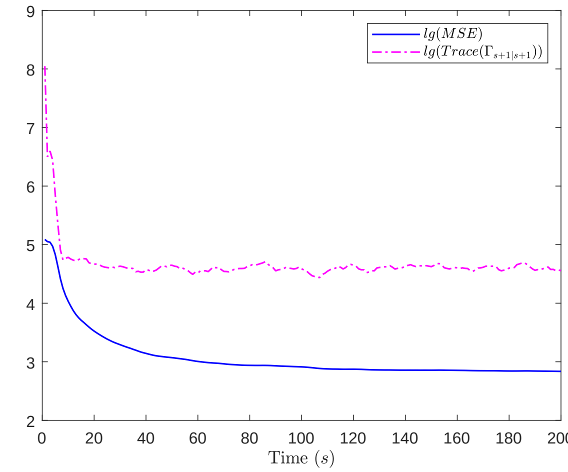

Fig. 4: Trajectories of TMEE and MSE.

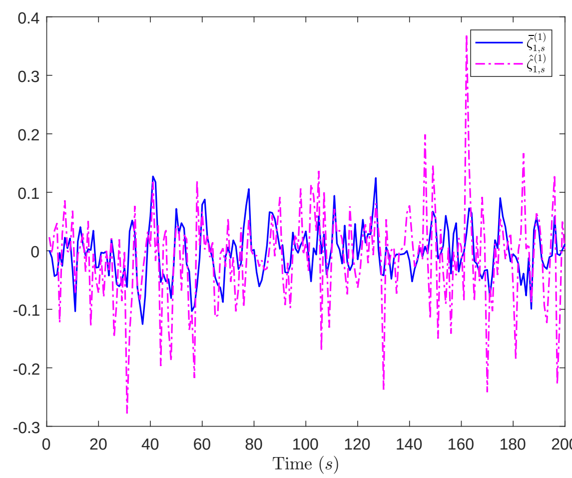

Fig. 5: Time-domain trajectories of the signal $\bar{\zeta}_{1,s}$ and its reconstructed signal $\hat{\zeta}_{1,s}$.

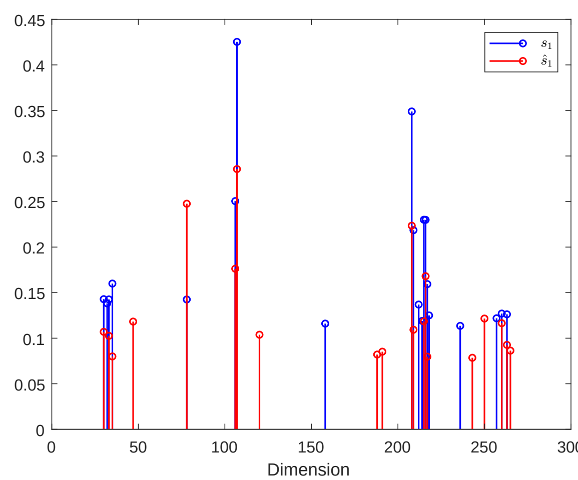

Fig. 6: Sparse-domain representations of s_1 and its reconstruction $\hat{s}_1$.

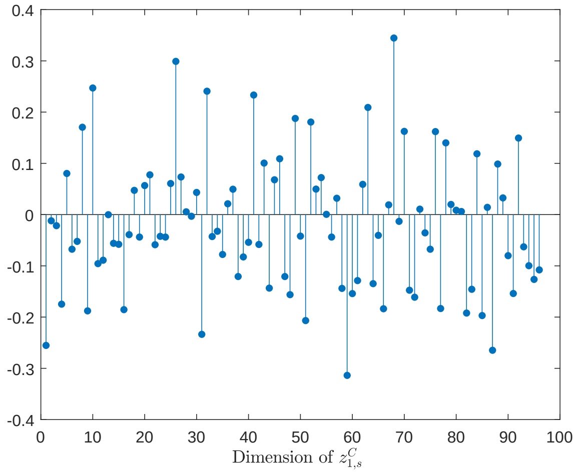

Fig. 7: Amplitude distribution of the compressed signal z_1^C.

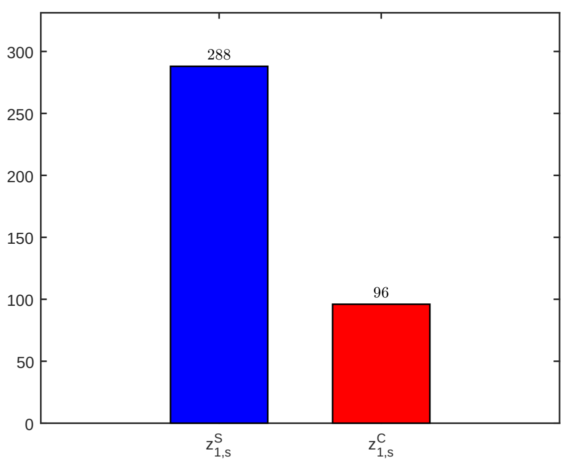

Fig. 8: Comparison of signal dimensions before and after CS-based compression.

uncertainty introduced into the CS recovery process by random channel fading, the impact mechanism of channel statistics on the recovery error has been thoroughly investigated, and a robust error model has been accordingly established. A state estimator has then been designed to counteract such uncertainty. By taking into account the recovery error induced by CS techniques, an upper bound on the estimation error for the designed estimator has been derived, and the estimator parameters have been obtained by minimizing this upper bound. Finally, simulation studies based on a USV-MADPS have been conducted to verify the effectiveness of the proposed approach in preserving estimation accuracy and robustness while reducing communication overhead.

Several research directions may be further pursued in future work. One promising direction lies in extending the proposed framework to distributed secure state estimation problems for WSNs subject to hybrid cyber-attacks, such as deception attacks, denial-of-service attacks, and data tampering. Another meaningful direction is to investigate adaptive relay selection and dynamic resource allocation strategies, so that transmission power, compression ratio, and communication topology can be jointly optimized according to time-varying channel conditions and network energy budgets. It is also of practical interest to develop distributed estimation schemes for nonlinear or multi-rate systems under CF relay architectures, where stronger modeling flexibility would be required. In addition, experimental validation on real wireless sensing platforms may be conducted to further examine the practical applicability of the proposed method in complex networked environments.

References

[1] C. Bian, Y. Shao, H. Wu, E. Ozfatura and D. Gündüz, Process-and-forward: deep joint source-channel coding over cooperative relay networks, *IEEE Journal on Selected Areas in Communications*, vol. 43, no. 4, pp. 1118–1134, 2025.

[2] T. Bruns, S. Lehner, X.-M. Li, K. Hessner and W. Rosenthal, Analysis of an event of “parametric rolling” onboard RV “polarstern” based on shipborne wave radar and satellite data, *IEEE Journal of Oceanic Engineering*, vol. 36, no. 2, pp. 364–372, 2011.

[3] R. Caballero-Águila, M. P. Frías-Bustamante and A. Oya-Lechuga, Least-squares linear estimation for multirate uncertain systems subject to DoS attacks, *International Journal of Network Dynamics and Intelligence*, vol. 4, no. 2, art. no. 100014, Jun. 2025.

[4] R. Caballero-Águila, A. Hermoso-Carazo and J. Linares-Pérez, Networked distributed fusion estimation under uncertain outputs with random transmission delays, packet losses and multi-packet processing, *Signal Processing*, vol. 156, pp. 71–83, 2019.

[5] E. J. Candès, The restricted isometry property and its implications for compressed sensing, *Comptes Rendus Mathematique*, vol. 346, pp. 589–592, 2008.

[6] F. Cao, F. Jia and X. He, Sensor fault detection and diagnosis of linear parabolic PDE systems with unknown inputs, *IEEE Transactions on Automatic Control*, vol. 69, no. 2, pp. 1014–1021, Feb. 2024.

[7] V. Cevher, Learning with compressible priors, *Advances in Neural Information Processing Systems*, vol. 22, pp. 261–269, 2009.

[8] W. Chen, J. Hu, Z. Wu and S. Ma, A survey on fault detection for networked systems under communication constraints, *Systems Science & Control Engineering*, vol. 13, no. 1, art. no. 2460434, 2025.

[9] Y. Chen, W. Wang and J. Xu, Robust H_∞ estimation for 2D FMLSS systems under asynchronous multi-channel delays: a partition reconstruction approach, *International Journal of Network Dynamics and Intelligence*, vol. 4, no. 3, art. no. 100017, Sept. 2025.

[10] T. Cover and A. E. Gamal, Capacity theorems for the relay channel, *IEEE Transactions on Information Theory*, vol. 25, no. 5, pp. 572–584, 1979.

[11] D. L. Donoho, Compressed sensing, *IEEE Transactions on Information Theory*, vol. 52, no. 4, pp. 1289–1306, 2006.

[12] T. Fossen and J. Strand, Passive nonlinear observer design for ships using Lyapunov methods: full-scale experiments with a supply vessel, *Automatica*, vol. 35, pp. 3–16, 1999.

[13] T. I. Fossen, *Handbook of Marine Craft Hydrodynamics and Motion Control*, Chichester, U.K.: Wiley, 2011.

[14] Y. Gao, J. Hu, H. Yu, C. Jia and C. Chen, Variance-constrained H_∞ state estimation for time-varying delayed neural networks with random access protocol and sensor failures, *International Journal of Network Dynamics and Intelligence*, vol. 4, no. 3, art. no. 100019, Sept. 2025.

[15] Y. Guo and X. He, Active fault diagnosis for stochastic systems under accuracy-limited sensors, *IEEE Transactions on Instrumentation and Measurement*, vol. 73, art. no. 3521809, 2024.

[16] D. Gurve, D. Delisle-Rodriguez, T. Bastos-Filho, and S. Krishnan, Trends in compressive sensing for EEG signal processing applications, *Sensors*, vol. 20, no. 13, art. no. 3703, 2020.

[17] V. Guruswami and A. Vardy, Maximum-likelihood decoding of Reed-Solomon codes is NP-hard, *IEEE Transactions on Information Theory*, vol. 51, no. 7, pp. 2249–2256, July 2005.

[18] L.-Y. Hao, H. Zhang, T.-S. Li, B. Lin and C. L. P. Chen, Fault tolerant control for dynamic positioning of unmanned marine vehicles based on T-S fuzzy model with unknown membership functions, *IEEE Transactions on Vehicular Technology*, vol. 70, no. 1, pp. 146–157, 2021.

[19] A. Hasan, I. Kuncara, A. Widyotriatmo, O. Osen and R. T. Bye, Secure state estimation and control for autonomous ships under cyberattacks, *Systems Science & Control Engineering*, vol. 13, no. 1, art. no. 2518964, 2025.

[20] J. Hu, J. Li, C. Jia, X. Yi and H. Liu, A recursive method to encryption-decryption-based distributed set-membership filtering for time-varying saturated systems over sensor networks, *IEEE/CAA Journal of Automatica Sinica*, vol. 12, no. 5, pp. 1047–1049, May. 2025.

[21] J. Hu, J. Li, H. Yan and H. Liu, Optimized distributed filtering for saturated systems with amplify-and-forward relays over sensor networks: a dynamic event-triggered approach, *IEEE Transactions on Neural Networks and Learning Systems*, vol. 35, no. 12, pp. 17742–17753, 2024.

[22] C. Huang, S. Coskun, H. R. Karimi and W. Ding, A distributed state and fault estimation scheme for state-saturated systems with quantized measurements over sensor networks, *Information Fusion*, vol. 110, art. no. 102452, 2024.

[23] C. Huang, L. Zhu, P. Mei, S. Coskun and S. Yang, Distributed state estimation over wireless sensor networks against deception attacks: a buffer-aided strategy, *IEEE Transactions on Consumer Electronics*, vol. 71, no. 3, pp. 8553–8561, Aug. 2025.

[24] U. Jayasankar, V. Thirumal, and D. Ponnurangam, A survey on data compression techniques: from the perspective of data quality, coding schemes, data type and applications, *Journal of King Saud University - Computer and Information Sciences*, vol. 33, no. 2, pp. 119-140, 2021.

[25] H. Katayama and H. Aoki, Straight-line trajectory tracking control for sampled-data underactuated ships, *IEEE Transactions on Control Systems and Technology*, vol. 22, no. 4, pp. 1638–1645, 2014.

[26] W. Le, B. Shen, L. Zou, J. Sun, Stubborn state estimation for time-delay systems with relay communication network: the half-duplex case, *Journal of the Franklin Institute*, vol. 362, no. 2, art. no. 107465, Jan. 2025.

[27] J. Li, R. Caballero-Águila, J. Hu and J. Linares-Pérez, Recursive estimation with compensation strategies under random access protocol and deception attacks, *IEEE Transactions on Signal Processing*, vol. 73, pp. 1954–1965, 2025.

[28] L. Li, Y. Du, Y.-H. Liu and H. Yang, Research on image compression encoding based on fixed dictionary, *Systems Science & Control Engineering*, vol. 13, no. 1, art. no. 2437160, 2025.

[29] Z. Li, T. Moan, K. Riska and B. Su, Heading control for turret-moored vessel in level ice based on Kalman filter with thrust allocation, *Journal of Marine Science and Technology*, vol. 18, pp. 460–470, 2013.

[30] C. Liang, D. He and C. Xu, Distributed H_∞ moving horizon estimation over energy harvesting sensor networks, *International Journal of Systems Science*, vol. 56, no. 15, pp. 3743–3757, 2025.

[31] G. Lyu and X. He, Distributed secure state estimation and attack detection for dynamical systems with attacks on a time-varying sensor set, *IEEE Transactions on Cybernetics*, vol. 55, no. 11, pp. 5151–5160, Nov. 2025.

[32] J. R. Magnus and H. Neudecke, *Matrix Differential Calculus with Applications in Statistics and Econometrics, 3rd ed*, Hoboken, NJ, USA: John Wiley & Sons, Inc., 2019.

[33] M. G. El-Mashed, Compressed sensing Kalman filter estimation scheme for MIMO system under phase noise problem, *IET Communications*, vol. 14, no. 22, pp. 4108–4115, 2020.

[34] X. Meng, H. Wang, Y. Li and Y. Shen, Unscented Kalman filtering for nonlinear systems with stochastic nonlinearities under FlexRay protocol, *International Journal of Network Dynamics and Intelligence*, vol. 4, no. 2, art. no. 100010, Jun. 2025.

[35] T. Pan, Y. Yuan, Z. Wang and X. Li, A region-based relay pursuit scheme for a pursuit-evasion game with curvature-bound players, *IEEE Transactions on Industrial Electronics*, vol. 71, no. 12, pp. 16308–16316, Dec. 2024.

[36] M. Shi, L. Ma and X. Yi, Recursive state estimation for complex networks with energy harvesting constraints and decode-and-forward relays, *IEEE Transactions on Systems, Man, and Cybernetics: Systems*, vol. 55, no. 8, pp. 5491–5502, 2025.

[37] D. Sivaraman, B. M. Pillai, C. Wiratkapun, J. Suthakorn and S. Ongwattanakul, Dynamic order selection analysis in adaptive polynomial Kalman filtering: implementation and integration of sensor data and hybrid image processing for bio-inspired needle systems, *Systems Science & Control Engineering*, vol. 13, no. 1, art. no. 2546839, 2025.

[38] J. Song, Z. Wang, Q. Liu and X. He, Remote state estimation for nonlinear systems under compression-decompression mechanism: a modified unscented Kalman filtering approach, *IEEE Transactions on Automatic Control*, vol. 71, no. 1, pp. 91–106, Jan. 2026.

[39] J. Sun, B. Shen, C. Wen and Y. Liu, Recursive state-fault filtering for stochastic nonlinear systems over sensor networks with sensor resolution and time-correlated fading channels, *Journal of the Franklin Institute*, vol. 362, no. 15, art. no. 108020, Oct. 2025.

[40] S. Sun, D. Chen, J. Hu and N. Yang, Event-triggered set-membership state estimation for discrete delayed linear systems over sensor networks, *Circuits, Systems, and Signal Processing*, vol. 43, pp. 4813–4835, May. 2024.

[41] Y.-C. Sun, K. Gao, L. Chen, F. Yang and L. Yao, Optimal power schedule for distributed Kalman filtering under DoS attacks: a Stackelberg game strategy, *International Journal of Systems Science*, vol. 56, no. 9, pp. 2067–2081, 2025.

[42] Z. Sun and C. Han, Linear state estimation for multi-rate NCSs with multi-channel observation delays and unknown Markov packet losses, *International Journal of Network Dynamics and Intelligence*, vol. 4, no. 1, art. no. 100005, Mar. 2025.

[43] E. Tian, M. Fan, L. Ma and D. Yue, Stochastic important-data-based attack power allocation against remote state estimation in sensor networks, *IEEE Transactions on Automatic Control*, vol. 70, no. 3, pp. 2012-2019, Mar. 2025.

[44] W. Wang, X. Kan, D. Ding, H. Liu and X. Gao, Distributed correntropy Kalman filtering over sensor networks with FlexRay-based protocols, *International Journal of Systems Science*, vol. 56, no. 6, pp. 1347–1359, 2025.

[45] P. Wen, H. Dong, F. Huo, J. Li, X. Lu, Observer-based PID control for actuator-saturated systems under binary encoding scheme, *Neurocomputing*, vol. 499, pp. 54–62, 2022.

[46] N. Zhang and J. Liang, Distributed interval fusion filtering for multirate nonlinear positive systems under amplify-and-forward relay: the finite-horizon case, *Information Fusion*, vol. 129, art. no. 104061, May. 2026.

[47] J. Zhang, G. Wei, D. Ding and Y. Ju, Distributed sequential state estimation over binary sensor networks with inaccurate process noise covariance: a variational Bayesian framework, *IEEE Transactions on Signal and Information Processing over Networks*, vol. 11, pp. 1–10, 2025.

[48] W. Zhang, Y. Zhao, H. Wang and Z. Yang, Robust model predictive control for polyhedral uncertain systems under relay and redundancy protocol, *International Journal of Systems Science*, vol. 56, no. 8, pp. 1617–1632, 2025.

[49] Y.-L. Zhi, Y.-Y. Wu, Y. Zhang and G. Yang, A new result on reachable set estimation for Markovian jump neural networks with time-varying delays, *International Journal of Systems Science*, vol. 56, no. 16, pp. 4131–4143, 2025.

[50] Y. Zhu, H. Zhang, E. Tian, W. Si and W. Zheng, Optimal DoS attack policy against periodically switched system with two-hop relay networks, *International Journal of Robust and Nonlinear Control*, vol. 35, no. 10, pp. 4318–4328, 2025.

[51] L. Zou, B. Song, J. Suo, N. Li and C. Wang, A survey on outlier-resistant state estimation and its applications, *Systems Science & Control Engineering*, vol. 13, no. 1, art. no. 2474471, 2025.

Pengyu Wen was born in Daqing, China, in 1995, and received his B.S. degree in Automation from Taiyuan University of Technology, Taiyuan, China, in 2018. He is now pursuing the Ph.D. degree in Petroleum and Natural Gas Engineering at Northeast Petroleum University, Daqing, China, and his research interests include wireless sensor networks, communication protocols and state estimation.

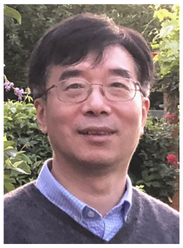

Zidong Wang (Fellow, IEEE) received the B.Sc. degree in mathematics in 1986 from Suzhou University, Suzhou, China, and the M.Sc. degree in applied mathematics in 1990 and the Ph.D. degree in electrical engineering in 1994, both from Nanjing University of Science and Technology, Nanjing, China.

He is currently Professor of Dynamical Systems and Computing in the Department of Computer Science, Brunel University of London, U.K. From 1990 to 2002, he held teaching and research appointments in universities in China, Germany and the UK. Prof. Wang's research interests include dynamical systems, signal processing, bioinformatics, control theory and applications. He has published a number of papers in international journals. He is a holder of the Alexander von Humboldt Research Fellowship of Germany, the JSPS Research Fellowship of Japan, William Mong Visiting Research Fellowship of Hong Kong.

Prof. Wang serves (or has served) as the Editor-in-Chief for *International Journal of Systems Science*, the Editor-in-Chief for *Neurocomputing*, the Editor-in-Chief for *Systems Science & Control Engineering*, and an Associate Editor for 12 international journals including IEEE Transactions on Automatic Control, IEEE Transactions on Control Systems Technology, IEEE Transactions on Neural Networks, IEEE Transactions on Signal Processing, and IEEE Transactions on Systems, Man, and Cybernetics-Part C. He is a Member of the Academia European, a Member of the European Academy of Sciences and Arts, an Academician of the International Academy for Systems and Cybernetic Sciences, a Fellow of the IEEE, a Fellow of the Royal Statistical Society and a member of program committee for many international conferences.

Hongli Dong (Senior Member, IEEE) received the Ph.D. degree in control science and engineering from the Harbin Institute of Technology, Harbin, China, in 2012. From 2009 to 2010, she was a Research Assistant with the Department of Applied Mathematics, City University of Hong Kong, Hong Kong. From 2010 to 2011, she was a Research Assistant with the Department of Mechanical Engineering, The University of Hong Kong, Hong Kong. From 2011 to 2012, she was a Visiting Scholar with the Department of Information Systems and Computing, Brunel University London, London, U.K. From 2012 to 2014, she was an Alexander Von Humboldt Research Fellow with the University of Duisburg-Essen, Duisburg, Germany. She is currently a Professor with Artificial Intelligence Energy Research Institute, Northeast Petroleum University, Daqing, China. She is also the Director of the Heilongjiang Provincial Key Laboratory of Networking and Intelligent Control, Daqing, China. Her current research interests include robust control and networked control systems. Professor Dong is an active reviewer of many international journals.

Weihao Song (Member, IEEE) received the B.S. degree in flight vehicle design and engineering in 2016 and the Ph.D. degree in aeronautical and astronautical science and technology in 2021, both from Beijing Institute of Technology, Beijing, China.

From May 2019 to May 2020, he was a Visiting Scholar with the Department of Computer Science, Brunel University of London, Uxbridge, U.K. Since 2021, he has been a Postdoctoral Researcher at Peking University. He is also currently an Honorary Research Fellow with the Department of Computer Science, Brunel University of London, Uxbridge, U.K. His research interests include Bayesian state estimation, distributed state estimation, nonlinear filtering, and networked control systems.